Green Chemistry

RSC Publishing

PAPER

View Article Online
View Journal | View Issue

Cite this: *Green Chem.*, 2013, **15**, 749

Efficient microalgae harvesting by organo-building blocks of nanoclays†

Wasif Farooq,[a] Young-Chul Lee,*[b] Jong-In Han,[b] Cornelius Hanung Darpito,[a] Minkee Choi[c] and Ji-Won Yang*[a]

Received 8th November 2012,
Accepted 16th January 2013

DOI: 10.1039/c3gc36767c

www.rsc.org/greenchem

The synthesis of aminoclays with Mg^{2+} or Fe^{3+}, placed in metal centers by sol–gel reaction with 3-aminopropyltriethoxysilane (APTES) as a precursor, is demonstrated, producing $-(CH_2)_3NH_2$ organo-functional pendants which are covalent-bonding onto cationic metals. The protonated amine groups in aqueous solution lead the efficient sedimentation (harvesting) of microalgae biomass within approximately 5 min and 120 min for fresh and marine species, respectively. To our surprise, the aminoclays did not depend on microalgae species or media for microalgae harvesting. In particular, the harvesting efficiency (%) of microalgae was not decreased in a wide pH region. The harvesting mechanism can be explained by the sweep flocculation of microalgae, which is confirmed by measurement of zeta potential of aminoclay in aqueous solution where aminoclay shows a positively charged surface in a wide pH region. In order to reduce the cost of aminoclays and to make the harvesting procedures simple, the membrane process using aminoclay-coated cotton filter is introduced for the treatment of 1 L-scale microalgae stocks. It is successfully performed with three recycles using the same aminoclay-coated cotton filter after removing the harvested microalgae biomass. Conclusively, the aminoclay-based microalgae harvesting systems are a promising means of reducing the cost of downstream processes in microalgae-based biorefinery.

Introduction

Since 2000, microalgae biomass, regarded as a third-generation feedstock, has become increasingly attractive within both academia and the industrial sector for its applicability to sustainable biodiesel production.[1–4] This non-grain feedstock has, relative to other crops, many advantages such as decreased land usage and significantly lower carbon dioxide (CO_2) emissions.[5–8] This seemingly ideal source material, however, has a number of problems that need to be resolved before it can become the feedstock of choice.[9–12]

A microalgae-based biorefinery encompasses various downstream processes, among which are cultivation, harvesting, drying, and extraction of targeted biomolecules including proteins, carbohydrates, and lipids.[13–19] The unit cost of each of these bioprocess steps has to be substantially reduced, and in fact a great number of research groups worldwide have devoted every effort to that end. One such area of endeavor is the development of economically viable harvesting techniques. The current techniques, none of which are as yet economically feasible, include centrifugation, flocculation using inorganic coagulants and organic flocculants, gravity sedimentation, filtration and screening, flotation, and electrophoresis methods.[20]

In 1997, organophyllosilicates (organoclays) with direct functional organic groups such as amino, thiol, phenol, hydroxyl, *etc.*, and backboned cationic metals (*e.g.*, Mg, Ca, Al, Cu, Ni, and Zn, *etc.*) have been developed under ambient conditions by sol–gel reaction.[21–27] Usually, 3-aminopropyl-functionalized magnesium phyllosilicate (aminoclay) is formed in aqueous solution as organo-building blocks by repulsion force of protonated amine groups. These organo-building blocks with a strong positive charge constructed a plethora of novel bio(nano)composites, with unique properties, enhanced mechanical and thermal stability while maintaining their intrinsic characteristics *via* self-assembly protocols such as wrapping of DNA, lipid, enzymes, and controlled drug release in the mesolamellar organic–inorganic structures;[28,29] additionally, they can preconcentrate, by electrostatic attraction, various heavy metals or useful ionic nutrients in aqueous solution.[30,31] Recently, such organoclays, functioning with primary amino sites, were expanded in design using other cationic metals (*e.g.*, Fe^{3+}, Sn^{4+}, and Mn^{2+}) in place of the usual Mg^{2+}. For

[a]*Advanced Biomass R & D Center, KAIST, 291 Daehakno, Yuseong-gu, Daejeon 305-701, Republic of Korea. E-mail: jwyang@kaist.ac.kr; Fax: +82-42-350-3924; Tel: +82-42-350-3910*
[b]*Department of Civil and Environmental Engineering (BK21 program), KAIST, 291 Daehakno, Yuseong-gu, Daejeon 305-701, Republic of Korea. E-mail: dreamdbs@kaist.ac.kr; Fax: +82-42-350-3698; Tel: +82-42-350-3610*
[c]*Department of Chemical and Biomolecular Engineering, KAIST, 291 Daehakno, Yuseong-gu, Daejeon 305-701, Republic of Korea*
†Electronic supplementary information (ESI) available. See DOI: 10.1039/c3gc36767c

example, usage of Fe^{3+}, which imparts a dual functionality, generates reactive oxygen species (ROS) in the presence of hydrogen peroxide (H_2O_2).[32] Although aminoclays have been reported (*e.g.*, magnesium in the center surrounded by 3-aminopropyl functional groups), to the present authors' knowledge, research on microalgal biorefinery using aminoclays as a novel flocculant for facile and effective microalgae harvesting has not yet been investigated. As a result, this unique property of aminoclay in the microalgae harvesting process drives us to destabilize cells, resulting in sweep flocculation.[14,33,34]

In this context, utilization of aminoclays (having high-density amino sites ($-NH_2$) and water-soluble, transparent, and less ecotoxic effects in aqueous solution[35]) for rapid harvesting of freshwater and marine microalgae is a challenging task. Biodiesel production from microalgae grown on spent media after harvesting might represent a promising approach to make the use of microalgae feedstocks economically viable.

Experimental methods

Preparation of aminoclays and aminoclay-coated fabrics

Each aminoclay (Mg-APTES clay and Fe-APTES clay) was synthesized according to the methodology available in the literature:[32] Briefly, 8.4 g (~0.04 mol) of $MgCl_2{\cdot}6H_2O$ (Junsei, Japan) or 10.8 g (~0.04 mol) of $FeCl_3{\cdot}6H_2O$ (Sigma-Aldrich, USA) was added to 200 mL of ethanol solution (95%) obtained from Samchun Pure Chemicals (Pyungtack, Korea). Following dissolution by 10 min of stirring, 13 mL (~0.06 mol) of 3-aminopropyltriethoxysilane (APTES, Sigma-Aldrich, USA) was pipetted into the magnesium chloride or ferric chloride ethanolic solution, which was then magnetically stirred overnight. The precipitated product (*i.e.*, Mg-APTES or Fe-APTES clay) was centrifuged (2800 rpm, 15 min) and subsequently collected. The products were washed twice with ethanol to remove excess cationic metals and oven-dried at 45 °C for 24 hours.

For fabric coating with Fe-APTES clay, cut fabrics (110 mm × 65 mm, length × width), purchased from a traditional Korean market in Daejeon were soaked in a dip tray containing 10.8 g (~0.04 mol) of $FeCl_3{\cdot}6H_2O$ in ethanol solution for six hours. The fabrics, after removal from the tray, were immersed overnight in 200 mL of ethanolic solution consisting of 40 mL (~0.18 mol) of APTES and 5 mL (~0.024 mol) of tetraethyl orthosilicate (TEOS, Sigma-Aldrich, USA), and marked "run = 1". "Run = 2" represented double-coating performance. After the coating process, the prepared fabrics were washed with pure ethanol and dried at room temperature for 24 hours.

Microalgae strains, growth conditions, and re-culture

The freshwater microalgae *Chlorella vulgaris* (UTEX-265) was purchased from the University of Texas (UTEX) Algae Collection Center (Texas, USA) and cultivated in standard TAP or standard F/2 media under a light intensity of 2000 lux. The marine species *Nannochloris oculata* (KMMCC-16), provided by the Korean Marine Culture Collection (Busan, Korea), was cultivated in standard F/2 media and supplied with 2% CO_2 under a light intensity of 2000 lux. The cyanobacteria species *Synechocystis* sp. PCC6803 was obtained from Chungnam National University (Daejeon, Korea). All three microalgae strains were cultivated in 500 mL flasks under 30 °C temperature and 125 rpm stirring-speed conditions. All of the apparatuses and media were autoclaved (121 °C for 15–20 min) before cultivation to ensure an aseptic environment. At the end of the log phase, biomass was collected for harvesting experiments. In order to determine the biomass concentration in the culture, the optical density of *Chlorella vulgaris*, *Nannochloris oculata*, and *Synechocystis* sp. was measured at 682, 680, and 730 nm,[36] respectively. Usually optical density for *Chlorella vulgaris* and *Nannochloris oculata* growth were measured from 660 nm to 680 nm. Batch-mode harvesting experiments were completed in a 100 mL glass cylinder or a 1 L glass beaker. To re-culture microalgae after harvesting, 50% TAP media was used to ensure the presence of 50% supernatant and 50% TAP media, with and without the addition of 1% (v/v) inoculum. Due to a fast growth and quick process to stationary phase of microalgae quickly, TAP media were used for the purpose of harvesting works.[37]

Bulk microalgae harvesting and filtration harvesting process

Bulk harvesting of microalgae by Mg-APTES clay was performed in a 1 L glass cylinder. The clay was mixed with microalgal culture for 1–2 min and then cultured to allow for flocculation. Supernatant samples were taken periodically to measure the density of the culture and to calculate the harvesting efficiency. The sample was removed from the middle of the glass cylinder and along the height of the cylinder. Fe-APTES clay deposited onto cotton fabric was used as a filter, according to the dead-end filtration system configuration. A total of 1.0 L of culture was used to test the harvesting performance, and the permeate weight was measured to calculate the flux through the filter. Harvesting and filtration efficiencies were measured using the equation

$$\text{Efficiency } (\%) = \left[1 - \frac{\text{OD}_\text{f}}{\text{OD}_\text{i}}\right] \times 100$$

where OD_f and OD_i are the final and initial optical densities of the culture, respectively.

The flux across the fabric filter was calculated as

$$\text{flux } (\text{L m}^{-2}\ \text{h}) = \text{volume of permeate/area time}$$

where the effective area of the Fe-APTES clay-coated cotton membrane was 71.50 cm^2. All experiments were conducted in duplicate and the average taken.

Conversion of extracted of microalgal lipids (oil) into fatty acid methyl ester (FAME, called biodiesel)

Biomass was centrifuged at 5000 rpm for 10 min at 4 °C and the supernatant was discarded and subsequently followed by rising with deionized water. Centrifuged biomass was frozen using liquid nitrogen and vacuum freeze dried at −40 °C. The total lipids were extracted using 10 mg of lyophilized biomass

with chloroform–methanol (2 : 1, v/v) solvent mixture similar to the Folch's method.[38] Extracted lipids were converted to fatty acid methyl esters (FAMEs) by transesterification reaction. Briefly, methanol was added to the extracted lipid with sulfuric acid as a catalyst and transesterification reaction occurred for 10 min at 100 °C. After reaction, 1 mL of deionized water was added and organic phase was separated from the water phase by centrifugation at 4000 rpm for 10 min. The FAMEs in the organic phase were analyzed by gas chromatography (GC, HP5890, Agilent, USA) with a flame ionized detector (FID) with equipped INNOWAX capillary column (30 m × 0.32 mm × 0.5 μm, Agilent, USA). The GC column temperature was programmed as follows: (1) initial column temperature at 50 °C, hold for 1 min, (2) increase to 200 °C at a rate of 15 °C min^{-1}, hold for 9 min, (3) increase to 250 °C at a rate of 2 °C min^{-1}, maintain for 2 min. Each FAME component was identified and quantified by comparing the retention times and peak areas with those of the FAME standard solutions.

Characterization and instruments

The microalgae biomass concentration (g L^{-1}) was calculated by measuring the optical densities (OD) with a UV-visible spectrophotometer (Beckman Coulter, DU 730) (see ESI, Fig. S1†). The morphologies of the microalgae and flocculated microalgae were examined under bright optical microscopy (Leica, model DM2500) and field-emission scanning electron microscopy (FE-SEM, Magellan 400, FEI). Air-dried aminoclay samples and aminoclay-coated fabrics were analyzed under transmission electron microscopy (TEM, JEM-2100F) and SEM micrographs with energy dispersive X-ray spectroscopy (EDX, Bruker) and video microscopy (EGVM-13M), respectively. All photographic images were captured with an iPhone digital camera. Powder X-ray diffraction (XRD) patterns were assessed by D/MAX-RB (Rigaku, 12 kW). Fourier transform infrared (FT-IR) spectra of KBr pellets (FTIR 4100) were recorded from 4000 cm^{-1} to 400 cm^{-1}. Zeta potential measurements were conducted with a Zetasizer Nano-ZS particle analyzer (Malvern). Quantitative analysis of silicon concentration in aqueous solution was performed by inductively coupled plasma atomic emission spectrometry (ICP-AES, Optima 7300 DV). The pH variation was monitored using a pH/ion meter (D-53, Horiba).

Results and discussion

Fundamental characteristics of aminoclays

In the present study, the prepared aminoclay was composed of a cationic metal center (Mg^{2+} or Fe^{3+}) presenting functional groups of $-(CH_2)_3NH_2$ organic pendants through covalent bonding (Scheme 1a). In aqueous solution, high-nitrogen-density protonated amine groups became positively charged and easily converted to delaminated organoclay sheets, thus resulting in a high-concentration transparent solution (100 mg mL^{-1}).[30] Transmission electron microscopy (TEM) micrographs of the aminoclays (Mg-APTES clay and Fe-APTES clay)

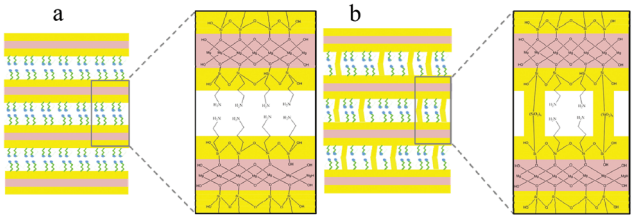

Scheme 1 (a) Ideal unit structure of Mg-APTES clay. (b) Unit structure as defected by sol–gel reaction with addition of tetraethyl orthosilicate (TEOS). Note that $FeCl_3$ instead of $MgCl_2$ was used to coat the aminoclay onto fabrics for naked-eye colorimetrical confirmation of aminoclay deposition.

dispersed in the aqueous solution indicated a broad sub-micrometer-diameter structure with polydisperse distributions (see ESI, Fig. S2a and S2b†) as well as a 50–100 nm-diameter structure with distinct contrasts (see ESI, Fig. S2c and S2d†). The morphology of those nanoparticles could be expected to interact with polysaccharide-based cell walls. The resulting X-ray diffraction (XRD) patterns of the aminoclays manifested basal spacing at d_{001} = 1.40 nm/1.60 nm at 2θ = 6.3°/5.7° and broad in-plane reflections at $d_{020,110}$ = 0.39 nm/0.40 nm at 2θ = 22.9°/22.5°, $d_{130,200}$ = 0.26 nm/0.26 nm at 2θ = 34.8°/34.3°, and $d_{060,330}$ = 0.16 nm/0.16 nm at 2θ = 59.4°/59.0° for respectively the Mg-APTES and Fe-APTES clay (see ESI, Fig. S3a and S3b†), which generally represent an amorphous phyllosilicate structure and 2 : 1 trioctahedral smectite reflection at 2θ = ~59°. The basal spacing at d_{001} exhibited the regular thickness of the layered structure, *i.e.*, talc-like phyllosilicate, which is in agreement with previous studies.[30,35] In addition to the identification of the crystalline structure and impurities in aminoclays, vibrations of functional groups in organic pendants of the aminoclays (see ESI, Fig. S4†) were characterized in both the Mg-APTES and Fe-APTES clay: –OH (3421 cm^{-1}), $-CH_2$ (3040 cm^{-1}), $-NH_3^+$ (2011 cm^{-1}), $-NH_2$ (1615 cm^{-1}), $-CH_2$ (1501 cm^{-1}), –Si–C– (1142 cm^{-1}), –Si–O–Si– (1035 cm^{-1}), –Mg–O– (410 cm^{-1}) and –Fe–O– (470 cm^{-1}).[30–32,35] The results indicated organic APTES immobilization onto cationic metal *via* coordination (covalent) bonding, eventually becoming layered aminoclays, as an amorphous organic–inorganic hybrid showing cationic building-block behaviors in aqueous solution with protonated amino groups of clay ($pK_a \approx 10.6$).[29]

Microalgae harvesting by aminoclays

Mg-APTES clay was used to harvest the freshwater microalgae species *Chlorella vulgaris* at a biomass concentration of 1.0 g L^{-1} (Fig. 1a). The addition of the aminoclay initiated flocculation and sedimentation within 5 min, which slowed down at 30 min, and stopped after 90 min. An Mg-APTES dose of 1.0 g L^{-1} was found to be optimal. Adsorption of microalgae cells on magnetite (Fe_3O_4) has been reported to occur within 5 min,[16] and similar results were obtained in the present investigation: at both 0.5 g L^{-1} and 1.0 g L^{-1} doses, cell settling was completed within 5 min, with no further increase in harvest efficiency (Fig. 1b). As the harvesting efficiency increased, the amounts of resulting fatty acid methyl ester

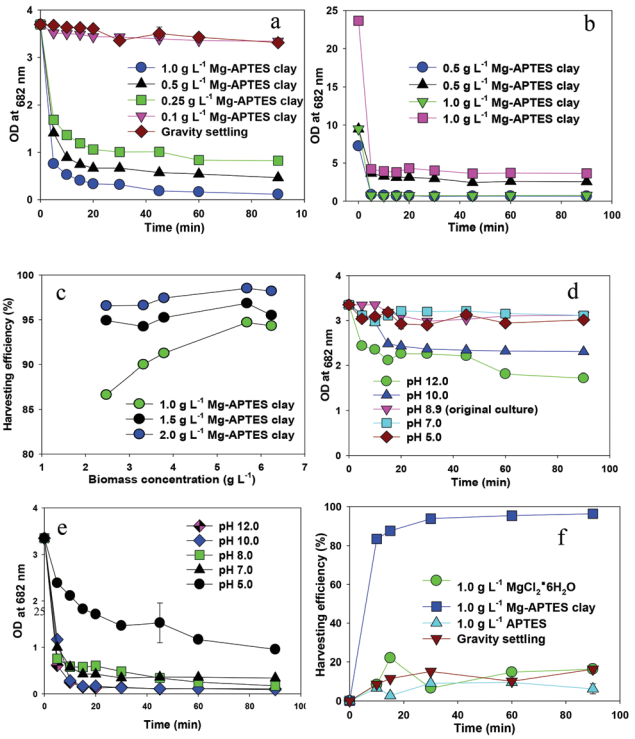

Fig. 1 (a) Harvesting of *Chlorella vulgaris* in freshwater by Mg-APTES clay dosage. (b) Effect of microalgae biomass stock concentration. (c) Harvesting efficiency (%) of *Chlorella vulgaris* according to biomass concentration (g L^{-1}) at 1.0 g L^{-1}, 1.5 g L^{-1}, and 2.0 g L^{-1} of Mg-APTES clay. (d) Effect of pH without clay treatment. (e) Effect of pH on *Chlorella vulgaris* harvesting at 1.0 g L^{-1} Mg-APTES clay treatment. (f) Harvesting efficiency with $MgCl_2$, Mg-APTES clay, APTES, and gravity settling for initial biomass concentration at 1.0 g L^{-1}.

(FAME, or biodiesel, mg g^{-1}) increased proportionally (see ESI, Fig. S5†), indicating that the harvesting step indeed plays a role in the overall efficiency of biodiesel production from microalgae biomass. Cell concentration along with Mg-APTES clay dosage appeared to affect the harvesting efficiency (Fig. 1c). The higher the initial microalgae, the lesser the aminoclay, possibly due to lengthened cell–cell bridge and the resulting sweep flocculation. In kinetics, the harvesting reactions according to Mg-APTES clay loading were predicted with the second-order model (see ESI, Table S1 and Fig. S6†).

The pH effect also was investigated (Fig. 1d). Surprisingly, cells were well settled down with 1.0 g L^{-1} of Mg-APTES clay within 5 min over a wide pH range (5.0–12.0). This unique feature proved to be quite useful, particularly in some pH-sensitive processes. The only exception was pH 5.0 (Fig. 1e): the high zeta potential of the microalgae cell surface at this low pH might result in a limited electrostatic interaction between Mg-APTES clay particles and microalgae cells. These aminoclays were worked in all microalgal culture conditions, which are different results, compared to conventional organic or inorganic coagulants with pH-sensitive actions.[14,20,33,34,39]

Even in control experiments without aminoclay (Fig. 1d), some degree of cell precipitation, called autoflocculation, occurred, particularly at pH values of 10.0 and 12.0. This was likely to happen, as, under alkaline conditions, the zeta potential of the microalgae cell surface is close to 0, and cells tend to be adsorbed onto precipitated $Mg(OH)_2$ from nutrient media.[18] Even so, it was considered that the use of pH changing as the sole harvesting means was insufficient. For confirmation, one additional control experiment, this one with clay precursors (*i.e.*, $MgCl_2{\cdot}6H_2O$ and APTES), was executed (Fig. 1f). Sure enough, Mg-APTES clay, not the precursors, exhibited the expected coagulation activity.

Fig. 2a–2d are microscopic images of coagulated microalgal cells with Mg-APTES clay. A bright optical microscopy image (Fig. 2a) revealed that aminoclay was surrounded by cells *via* cell grouping (aggregation; indicated by the white arrows). Interestingly enough, a few cells appeared to be disrupted (see black arrows); this might have occurred due to the instability of microalgal cell walls caused by the cationic characteristics of Mg-APTES clay. An SEM micrograph more clearly displayed this (Fig. 2c): the Mg-APTES clay seemed to serve as glue, making microalgal cells stick together. This effect can be seen even more clearly when compared with a microscopic image of microalgal cells without the aminoclay (Fig. 2d).

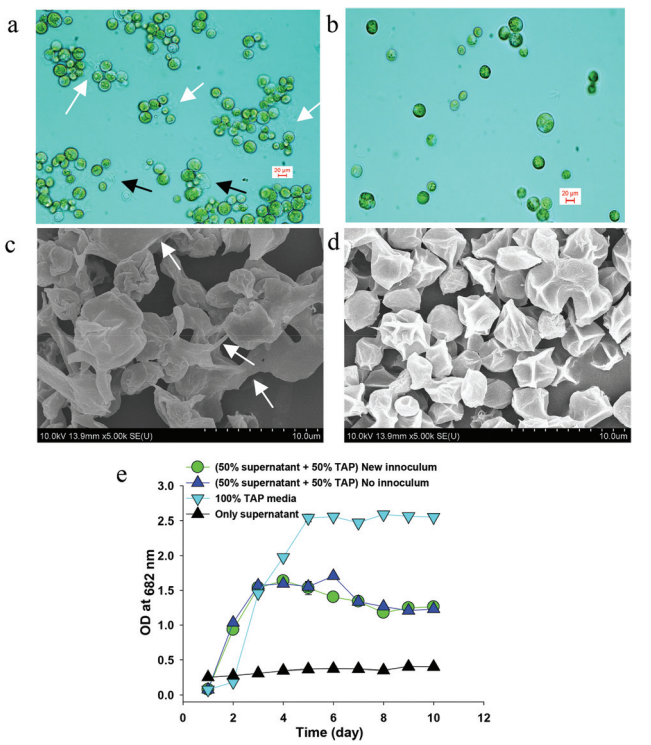

Fig. 2 (a) Optical micrograph of flocculated *Chlorella vulgaris* and Mg-APTES clay after harvesting process. The white arrows indicate flocculated Mg-APTES clay and *Chlorella vulgaris*, and the black arrows indicate disrupted microalgal cells. (b) Optical micrograph of fresh *Chlorella vulgaris*. (c) Scanning electron microscopy (SEM) image of flocculated *Chlorella vulgaris* and Mg-APTES clay after harvesting process. The white arrows indicate aminoclay materials linked with *Chlorella vulgaris*. (d) Scanning electron microscopy (SEM) image of fresh *Chlorella vulgaris*. (e) Reculturing of *Chlorella vulgaris* using supernatant after microalgae harvesting with 2.0 g L^{-1} of Mg-APTES clay for reuse of both water and residual Mg-APTES clay.

Table 1 Mg-APTES clay concentration treated and in supernatant after microalgae harvesting according to initial biomass concentration

Initial biomass (OD)	Treated Mg-APTES clay (g L^{-1})	Mg-APTES clay (g L^{-1}) in supernatant
2.0	0.5	0.4117
2.0	1.0	0.7889
2.0	2.0	1.6370
3.0	1.0	0.8419
3.0	2.0	1.6167
6.0	1.0	0.8541
6.0	2.0	1.7001

Regrowth of residual microalgae after harvesting

Unreacted aminoclay particles were quantified after harvesting (Table 1) by measurement of the aqueous Si concentration (see ESI, Fig. S7†). Up to 85% of added Mg-APTES clay was found to be left behind in the supernatant. Since it is of prime importance to make maximum use of aminoclay together with the growth medium to ensure the economical viability of microalgae-based fuel production, regrowth of microalgae in the spent medium after addition of 50% TAP media was attempted (Fig. 2e). The results showed that re-cultivation was possible even without an additional inoculum, though the final cell density was lower than in the 100% TAP media (Fig. 2e). This reduced growth might be attributable to the depletion of essential nutrients in the first cultivation rather than to the toxicity of the remaining aminoclay. In order to harvest cells from the second culture, however, additional aminoclay (approximately 0.15 g L^{-1}, data not shown) was needed.

Microalgae harvesting for broad-spectrum of species

To determine if aminoclay works for other species of microalgae, a freshwater cyanobacterium *Synechocystis* sp. and a marine organism *Nannochloris oculata* were also tested (see ESI, Fig. S8†). In the case of *Synechocystis* sp., only 0.25 g L^{-1} of Mg-APTES clay was sufficient, and with this low dosage harvesting was completed within 10 min (see ESI, Fig. S8a†). When 1.0 g L^{-1} of Mg-APTES was used, which was the optimal dosage for *Chlorella* sp., approximately 93% and 99% harvest efficiencies were obtained with the marine media containing 10 g L^{-1} and up to 30 g L^{-1} of sea salt, respectively (see ESI, Fig. S8b†). This result implied that this novel coagulant has selective advantages over common cationic polymer flocculants that are known to offer only limited harvesting efficiencies in high-salinity (>5 g L^{-1}) media.[20]

The overall experimental findings revealed that Mg-APTES clay has four main advantages over conventional coagulants/flocculants. First, Mg-APTES clay is dependent on neither species nor culture pH. Second, it produces only limited sludge, greatly reducing the necessity of wastewater treatment. Third, a culture medium with aminoclay is sufficiently transparent and shows limited toxicity to microalgae, making possible the recycling of both clay and medium. Finally, the basic property of aminoclay in spent media might accelerate the rate of CO_2 gas dissolution, which, along with light, is a critical growth factor in algal cultivation.

Mechanism study of microalgae harvesting

The flocculation mechanism by aminoclay, apparently an electrostatic interaction, can be explained in relation to the zeta potential of Mg-APTES clay and microalgae. Fig. 3a shows the zeta potential of Mg-APTES clay with respect to dosage: a significant increase of positive charge up to 2 g L^{-1}, followed by asymptotic saturation, ~+28 mV. The clay displayed a positive charge (greater than + 20 mV) over a wide, pH 4–10 range (Fig. 3b).[29]

Taking into consideration the importance of seawater-based microalgal cultivation in South Korea, two more marine species, *Chlorella vulgaris* and *Nannochloris oculata*, were tested in F/2 media of 30 g L^{-1} sea salt concentration (Fig. 3c and 3d). Approximately 0.25 g L^{-1} of Mg-APTES clay was required, but the harvesting time was prolonged to 120 min compared with freshwater species. In the absence of Mg-APTES clay, *Chlorella vulgaris* grown in the seawater medium showed an approximately 70% harvesting efficiency after 120 min (Fig. 3c), and *Nannochloris oculata* did not sediment at all, even after 200 min (Fig. 3d). With increases in the Mg-APTES clay dose (0, 0.25, 0.5, and 1.0 g L^{-1}), the zeta potential also increased, thereby leading to sweep flocculation.[20,39] In detail, as shown in zeta potential measurement that charge neutralization occurred, and as a result, coagulation by electrostatic bridging happened and large flocs settled. However, with increase in microalgal concentration (Fig. 1b), microalgal harvesting is independent of aminoclay concentration and big flocs sweep the suspended algae from the solution. Aminoclay concentration required for harvesting of algae did not increase with increase in algal biomass. This shows that two different flocculation mechanisms operated. At low algal concentration

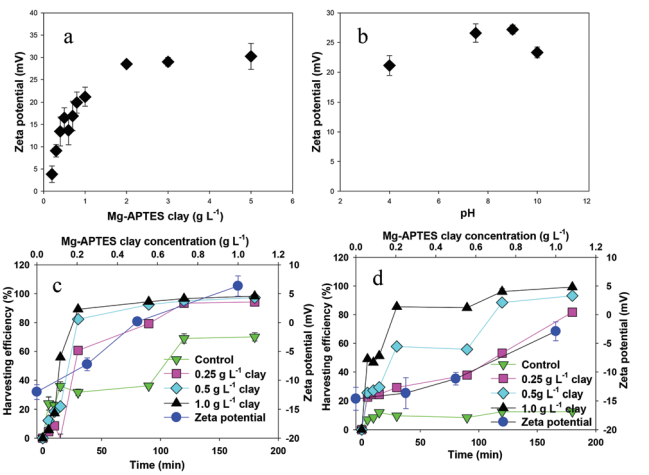

Fig. 3 (a) Zeta potential of Mg-APTES clay doses. (b) 1.0 g L^{-1} Mg-APTES clay according to pH of aqueous solution. (c) Harvesting efficiency (%) and zeta potential of Mg-APTES clay in supernatant of *Chlorella vulgaris* in F/2 media and (d) of *Nannochloris oculata* in F/2 media, at 30 g L^{-1} sea salt concentration after microalgae harvesting. In both (c) and (d), the control indicates gravity settling without Mg-APTES clay treatment.

the charge neutralization was proportional with the aminoclay concentration, while at high algal concentration the amount of aminoclay required did not increase. This means that electrostatic bridging followed by charge neutralization is not only mechanism.[14] Harvesting efficiency is dependent of aminoclay concentration (Fig. 1a), while at high concentration of algal cells (Fig. 1b) there is no correlation between algal cell concentration and dose of coagulants. This shows the presence of sweep flocculation.[34]

Microalgae harvesting using aminoclay-coated cotton filter in the application of membrane process

To improve the practicality of the aminoclay-based harvesting technique developed in this study, aminoclay-coated fabric was utilized as a filtration membrane. Water-soluble aminoclays were introduced to the membrane through tetraethyl orthosilicate (TEOS), an additive for sol–gel synthesis, in order to avoid delamination when in contact with water. They were then applied for repeated harvesting using 1 L of microalgae feedstocks. Aminoclay was immobilized onto fabrics by means of inducing a structural defect; thereby, delamination of the clay sheets in the aqueous solution was prevented (Scheme 1b), and the OH groups of each clay sheet of TEOS were cross-linked.[40] For this dual-end functionalization technique, nylon and cotton were selected as supporting fabrics, and coated (0, 1, and 2 runs) with another type of aminoclay (*i.e.*, Fe-APTES clay) according to a dipping protocol (see "Experimental methods" above), thus taking advantage of the various functional groups of the chosen fabrics and enabling easy deposition of aminoclay particles.[41] Fe-APTES clay was used instead of Mg-APTES clay in this particular experiment because Fe-based clay, which possesses similar characteristics to Mg-based clay and yet is of a brown color, offers a convenient way to monitor uniform deposition of clay particles in a sol–gel reaction (see ESI, Fig. S3 and S4†). Fig. 4a shows the Fe-APTES clay-coated cotton (runs = 2; 110 mm × 65 mm, L × W), which displays a uniform coating of aminoclay due to pore sizes sufficiently small to prevent passage of microalgae cells. This result, corresponding to the presence of Fe, Si, Cl, C, O, and N in the Fe-APTES clay composition (where Cl is a counter-anion stabilizing protonated $-NH_2$ sites; see ESI, Fig. S9†), was confirmed by energy-dispersive X-ray (EDX) microanalysis.[35] C and O come from both the aminoclay and cotton. Fe-APTES clay particles appeared to be distributed into the empty spaces of the cotton mesh for harvesting of microalgal cells. The performance of this Fe-APTES clay-coated cotton membrane was tested on a filtration system having a treatment capacity of 100 mL of microalgae feedstocks (Fig. 4b) according to the fabrics and dipping coating runs. The harvesting efficiency (%) was ~95% in both the cotton and nylon fabric systems (runs = 2; Fig. 4c and 4d), and the harvesting efficiency (>95%) in both cotton (runs = 2) and nylon (runs = 2) was achieved after 10 min. The flux (L m^{-2} h) was gradually decreased to ~55 (Fig. 4c and 4d) by biofouling film formation (see ESI, Fig. S10†). However, this flux was managed by gravity only in this study, that is, without application of external pressure.

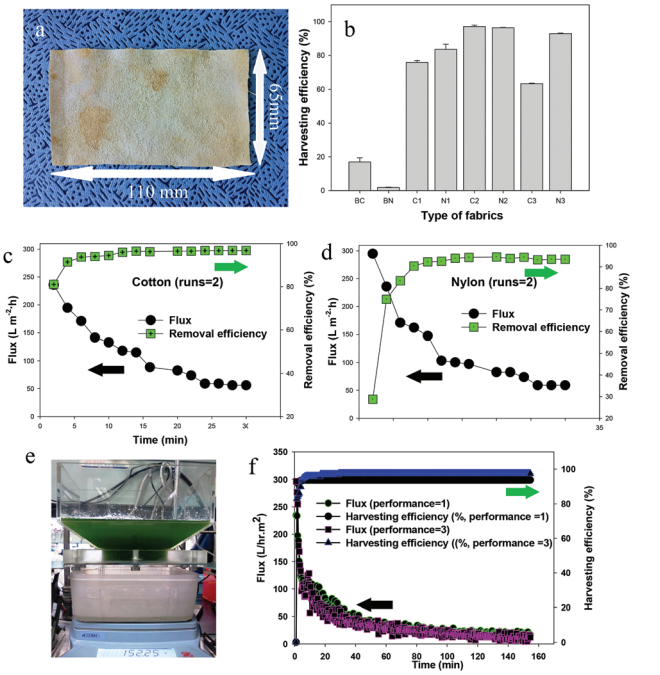

Fig. 4 (a) Photograph of Fe-APTES clay-coated cotton (runs = 2). (b) *Chlorella vulgaris* harvesting by filtration method with aminoclay (Fe-APTES clay)-coated fabrics. Note that BC, BN, C1, N1, C2, N2, C3, and N3 indicate blank cotton, blank nylon, cotton (run = 1), nylon (run = 1), cotton (runs = 2), nylon (runs = 2), cotton (runs = 3), and nylon (runs = 3), respectively. (c and d) Flux (L m^{-2} h) and removal efficiency (%) of microalgae harvesting with aminoclay-coated cotton membrane (runs = 2) (c) and aminoclay-coated nylon membrane (runs = 2) (d). (e) Photograph of 1 L microalgae feedstock and filtration system for harvesting of microalgae biomass. (f) Flux and removal efficiency (%) using aminoclay-coated cotton membrane as filter.

In order to scale up to the 1 L capacity, new filtration equipment was designed (see ESI, Fig. S11†). Comparing cotton and nylon fabrics as support matrices for aminoclay deposition, cotton was the more suitable and convenient choice, owing to its mechanical flexibility facilitating uniform coating, which advantage can be attributed to the versatile functions of cotton fibers. Three recycles with the aminoclay-coated cotton membrane (runs = 2) were successfully conducted (Fig. 4e and 4f). During 150 min of performance, 1 L of microalgae feedstocks was completed, the microalgae biomass was successfully harvested, and, after removal of that biomass, the recycle processes were performed three additional times using the same cotton membrane as a filter (see ESI, Fig. S12 and S13†). However, to enhance or maintain flux, additional vibration or vacuum modes would be necessary.[42,43] Thus, we are currently pursuing these works with consideration of effective membrane surface, flux rate, and recovery time of harvested biomass for tonnes scale.

Conclusions

In summary, the use of aminoclay as an efficient flocculant and of aminoclay-coated cotton as a filtration membrane in

the harvesting of microalgae biomass was demonstrated. These novel strategies were developed for application to both freshwater and marine microalgae species. The experimental results clearly showed that the aminoclay-based microalgae-harvesting systems are a promising means of reducing the cost of microalgae-based biorefinery in general and of downstream processes in particular. It is also believed that the use of aminoclay as a coating material, trialed in this study in the form of aminoclay-coated cotton belts, can offer the additional advantage of continuous harvesting.

Acknowledgements

W.F. and Y.-C.L. conceived the research idea; W.F., Y.-C.L. and C.H.D. performed the experiments; W.F., Y.-C.L., J.-I.H., M.C. and J.-W.Y. discussed the results; W.F., Y.-C.L. and J.-W.Y. wrote the paper. This work was supported by the Advanced Biomass R&D Center (ABC) as a Global Frontier Project funded by the Ministry of Education, Science and Technology (ABC-2010-0029728). We thank all of the members of the National NanoFab Center (NNFC) for the fruitful discussions on TEM and SEM imaging. We thank Kyochan Kim for the continuous flow measurement using Generic RS232 Communicator Ver. 05 and Jungmin Kim for the seed supply of *Nannochloris oculata*.

Notes and references

1 P. J. I. Williams, *Nature*, 2007, **450**, 478.
2 R. H. Wijffels and M. J. Barbosa, *Science*, 2010, **329**, 796.
3 P. Hunter, *EMBO Rep.*, 2010, **11**, 583.
4 R. H. Wijffels, M. J. Barbosa and M. H. M. Eppink, *Biofuels, Bioprod. Biorefin.*, 2010, **4**, 287.
5 R. Luque, L. Herrero-Davila, J. M. Campelo, J. H. Clark, J. M. Hidalgo, D. Luna, J. M. Marinas and A. A. Romero, *Energy Environ. Sci.*, 2008, **1**, 542.
6 R. Luque, *Energy Environ. Sci.*, 2010, **3**, 254.
7 P. M. Foley, E. S. Beach and J. B. Zimmerman, *Green Chem.*, 2011, **13**, 1399.
8 Y. C. Sharma, B. Singh and J. Korstad, *Green Chem.*, 2011, **13**, 2993.
9 H. Michel, *Angew. Chem., Int. Ed.*, 2012, **51**, 2516.
10 M. K. Lam and K. T. Lee, *Biotechnol. Adv.*, 2012, **30**, 673.
11 B.-H. Um and Y.-S. Kim, *J. Ind. Eng. Chem.*, 2009, **15**, 1.
12 N.-H. Norsker, M. J. Barbosa, M. H. Vermuë and R. H. Wijffels, *Biotechnol. Adv.*, 2011, **29**, 24.
13 D. Vandamme, S. C. V. Pontes, K. Goiris, I. Foubert, L. J. J. Pinoy and K. Muylaert, *Biotechnol. Bioeng.*, 2011, **108**, 2320.
14 N. B. Wyatt, L. M. Gloe, P. V. Brady, J. C. Hewson, A. M. Grillet, M. G. Hankins and P. I. Pohl, *Biotechnol. Bioeng.*, 2012, **109**, 493.
15 Z.-H. Yang, J. Huang, G.-M. Zeng, M. Ruan, C.-S. Zhou, L. Li and Z.-G. Rong, *Bioresour. Technol.*, 2009, **100**, 4233.
16 L. Xu, C. Guo, F. Wang, S. Zheng and C.-Z. Liu, *Bioresour. Technol.*, 2011, **102**, 10047.
17 D.-G. Kim, H.-J. La, C.-Y. Ahn, Y.-H. Park and H.-M. Oh, *Bioresour. Technol.*, 2011, **102**, 3163.
18 Z. Wu, Y. Zhu, W. Huang, C. Zhang, T. Li, Y. Zhang and A. Li, *Bioresour. Technol.*, 2012, **110**, 496.
19 Y.-L. Cheng, Y.-C. Juang, G.-Y. Liao, P.-W. Tsai, S.-H. Ho, K.-L. Yeh, C.-Y. Chen, J.-S. Chang, J.-C. Liu, W.-M. Chen and D.-J. Lee, *Bioresour. Technol.*, 2011, **102**, 82.
20 C.-Y. Chen, K.-L. Yeh, R. Aisyah, D.-J. Lee and J.-S. Chang, *Bioresour. Technol.*, 2011, **102**, 71.
21 S. Mann, S. L. Burkett, S. A. Davis, C. E. Fowler, N. H. Mendelson, S. D. Sims, D. Walsh and N. T. Whilton, *Chem. Mater.*, 1997, **9**, 2300.
22 J. Minet, S. Abramson, B. Bresson, C. Sanchez, V. Montouillout and N. Lequeux, *Chem. Mater.*, 2004, **16**, 3955.
23 M. G. da Fonseca, E. C. da Silva Filho, R. S. A. Machado Jr., L. N. H. Arakaki, J. G. P. Espinola and C. Airoldi, *J. Solid State Chem.*, 2004, **177**, 2316.
24 M. A. Melo Jr., F. J. V. E. Oliveira and C. Airoldi, *Appl. Clay Sci.*, 2008, **42**, 130.
25 M. G. da Fonseca and C. Airoldi, *J. Mater. Chem.*, 2000, **10**, 1457.
26 K. K. R. Datta, M. Eswaramoorthy and C. N. R. Rao, *J. Mater. Chem.*, 2007, **17**, 613.
27 M. Jaber, J. Miehé-Brendlé, M. Roux, J. Dentzer, R. L. Dred and J.-L. Guth, *New J. Chem.*, 2002, **26**, 1597.
28 S. Mann, *Nat. Mater.*, 2009, **8**, 781.
29 P. Chaturbedy, D. Jagadeesan and M. Eswaramoorthy, *ACS Nano*, 2010, **4**, 5921.
30 Y.-C. Lee, E. J. Kim, D. A. Ko and J.-W. Yang, *J. Hazard. Mater.*, 2011, **196**, 101.
31 Y.-C. Lee, E. J. Kim, H.-J. Shin, M. Choi and J.-W. Yang, *J. Ind. Eng. Chem.*, 2012, **18**, 871.
32 Y.-C. Lee, M. I. Kim, M.-A. Woo, H. G. Park and J.-I. Han, *Biosens. Bioelectron.*, 2013, **42**, 373.
33 D. Ghernaout and B. Ghernaout, *Desalin. Water Treat.*, 2012, **44**, 15.
34 A. Papazi, P. Makridis and P. Divanach, *J. Appl. Physiol.*, 2010, **22**, 349.
35 H.-K. Han, Y.-C. Lee, M.-Y. Lee, A. J. Patil and H.-J. Shin, *ACS Appl. Mater. Interfaces*, 2011, **3**, 2564.
36 M. Zhbanko, V. Zinchenko, M. Gutensohn, A. Schierhorn and R. B. Klösgen, *J. Bacteriol.*, 2005, **187**, 3071.
37 O. Perez-Garcia, F. M. E. Escalante, L. E. de-Bashan and Y. Bashan, *Water Res.*, 2011, **45**, 11.
38 S.-J. Park, Y.-E. Choi, E. J. Kim, W.-K. Park, C. W. Kim and J.-W. Yang, *Bioprocess Biosyst. Eng.*, 2012, **35**, 3.
39 N. Uduman, Y. Qi, M. K. Danquah, G. M. Forde and A. Hoadley, *J. Renewable Sustainable Energy*, 2010, **2**, 012701.
40 A. S. O. Moscofian, C. T. G. V. M. T. Pires, A. P. Vieira and C. Airoldi, *RSC Adv.*, 2012, **2**, 3502.
41 L. Bao and X. Li, *Adv. Mater.*, 2012, **24**, 3246.
42 S. H. Shuit, Y. T. Ong, K. T. Lee, B. Subhash and S. H. Tan, *Biotechnol. Adv.*, 2012, **30**, 1364.
43 G. Mezohegyi, M. R. Bilad and I. F. J. Vankelecom, *Bioresour. Technol.*, 2012, **118**, 1.